Electrophysiological Phenotype in Angelman Syndrome Differs Between Genotypes

Supplemental Information

Supplemental Methods and Materials

Data Collection

EEG recordings were obtained from patients with AS through the AS Natural History Study (ClinicalTrials.gov identifier: NCT00296764) between 2006 and 2014 recorded at two sites: 1) Rady Children's Hospital San Diego (RCHSD) (50 datasets from 30 unique participants) and 2) Boston Children's Hospital (BCH) (47 datasets from 34 unique participants). Consent was obtained from participating families according to the Declaration of Helsinki and was approved by the institutional review boards of BCH and the University of California San Diego (UCSD). A subset of AS data from RSCHD were previously analyzed by Sidorov and colleagues as part of a separate study (1). Data from both centers has been analyzed previously by Vendrame and collegues in terms of EEG abnormalities (2). EEG recordings from a control group of children with typical development (TD) were also obtained through BCH (56 participants, single recordings). All TD participants were children who had tested negative for neurological or developmental concerns. Groups were not age matched; however, this was accounted for appropriately using a linear mixed model (LMM, see below).

EEG data were acquired in a clinical setting using an international 10-20 EEG montage (19 channels). Some recordings included auxiliary channels such as electrooculogram (EOG) and electrocardiogram (ECG). All data were acquired using BioLogic and Xltek systems (Natus Medical Incorporated, Pleasanton, California; sampling rates: 200 Hz, 256 Hz, and 512 Hz). The awake state was not further controlled with respect to eye condition (e.g., eyes open or eyes closed) as the ages and developmental abilities of many participants precluded following instructions. Some EEGs included segments in which the participant was encouraged to sleep, as

well as light flash stimuli and hyperventilation intended to trigger epileptiform activity. Furthermore, segments of data during which the participant was drowsy were also indicated by the EEG tech. All such segments of data described above were excluded from analyses. Most data were collected from children. To minimize effects related to age extremes, we excluded 7 infants and adults by restricting the analyses to participants with ages between 12 – 216 months (1 - 18 years). 144 datasets entered preprocessing.

Preprocessing

Both the pediatric population and the loosely controlled clinical setting present challenges in the form of many physiological and technical artifacts and changes in the participant's state. A careful preprocessing was therefore essential to perform quantitative analyses. To this end, EEG data were bandpass filtered 0.5 – 45 Hz (FIR, filter order: 2 x sampling rate). Then, portions of unusable EEG data containing gross artifacts, including muscle bursts and technical artifacts, were identified by visual inspection and excluded from analysis. Furthermore, bad channels (i.e., flat or subject to frequent technical artifacts) were identified and excluded (number of bad channels per participant: 0.75 ± 0.82, mean ± std; range 0 – 3). For 10 datasets, the overall EEG data quality was considered insufficient for quantitative analysis. The artifact rejection was guided by inspection of EEG traces, physiological signals from auxiliary channels (EOG, electromyogram or EMG, proxy for EMG derived from >45 Hz power), and data annotations provided by the EEG technician during acquisition indicating the participant's behavioral state. Sections of data that included sleep, drowsiness, light flashes, and instructed hyperventilation were marked for exclusion. Additionally, all remaining data were manually screened for sleep-related EEG features and corresponding sections were excluded if present. Next, independent component analysis (ICA) was applied to remove remaining artifacts including eye blinks, saccades, ballistocardiogram, and muscle activity (FastICA algorithm (3, 4)); number of removed artefactual ICs: 5.26 ± 2.1, mean ± std; range: 0 – 9). Finally, rejected channels were interpolated and data were re-referenced to average.

The final dataset analyzed included 127 recordings from 106 participants. Three deletion AS participants (two atypical, one unknown deletion size) were excluded from the AS genotype

comparison to allow for testing of differences between deletion class I and class II. The individual length of useable data per dataset ranged from 2.82 – 41.3 minutes in length (15.9 ± 8.36 minutes, mean ± std), corresponding to 30 – 1003 frequency transform windows for the lowest frequency analyzed (see Frequency Transform; 259 ± 188 windows, mean ± std; 7 additional participants were excluded who had too little analyzable data, threshold: 25 analysis windows for lowest frequency analyzed, see Frequency Transform). See Supplemental Table S1 for a summary of retained data by genotype and testing site.

Frequency Transform

Power spectral estimates were derived for logarithmically scaled frequencies with a spectral smoothing of 1/3 octave ($f/\sigma_f = 8.7$) using Morlet Wavelets (5). This frequency transform accounts for the logarithmic nature of electrophysiological signals (6). Center frequencies were spaced logarithmically according to the exponentiation of the base 2 with exponents ranging from 0 (1 Hz) to 5 (32 Hz) in steps of 1/8. Power spectral estimates were derived as average power values of successive 3/4-overlapping temporal windows of continuous clean data. Absolute power values were then scaled and log-transformed to have units $10*\log_{10}(\mu V^2/\log_2(Hz))$. Consequently, differences between signals have units in decibels (dB). Furthermore, the power spectral density is based on $\log_2(Hz)$ rather than Hz to account for the logarithmic nature of electrophysiological signals (6). For analyses of relative power, data were expressed in units of $1/\log_2(Hz)$.

Peak Frequencies

To extract peak frequencies, we averaged power spectra across electrodes. Peak labeling was performed both automatically (using the local maximum) and manually (by visual inspection) within pre-defined frequency ranges (delta: 1.5 – 4 Hz; theta 4 – 8 Hz) for each visit of each participant with useable data. In instances where automatically- and manually-labeled peak frequencies agreed within 5%, the automatic peak label was used; otherwise, the manual peak label was used.

As an alternative measure for peak frequency, we used the "center of mass" within the pre-defined frequency ranges (from f_{min} (1.5 and 4 Hz, for delta and theta respectively) to f_{max} (4 and 8 Hz, respectively)), derived as the weighted average value of the frequency (f_i, i^{th} *frequency analyzed*). With $P(f_i)$ being the power spectral density (without log-scaling) at frequency f_i, the center of mass frequency derives as:

$$f_{center\ of\ mass} = \frac{\sum_{f_i=f_{min}}^{f_{max}} f_i \cdot P(f_i)}{\sum_{f_i=f_{min}}^{f_{max}} P(f_i)}$$

Statistical Analyses

For statistical analysis we used LMMs (7). The advantage of LMMs is the ability to model correlated data from longitudinal measurements by construction. We used the following LMM and variants thereof with less fixed factors:

P ~ 1 + GENOTYPE + AGE + GENOTYPE:AGE + (1|PARTICIPANT)

where P is log-transformed power in a given frequency band, AGE is the $\log_2$-transformed and mean-centered age, and GENOTYPE contains categorical variables [AS, TD], [deletion, non-deletion], or [deletion class I, deletion class II]. We use log-transformed age to account for the nonlinear rate of change in childhood development, i.e., faster developmental changes at younger ages.

We then used two approaches to derive p-values and confidence intervals. First, to derive 95% confidence intervals for illustration, and to test specific hypotheses, we used t-tests within LMM while using the Satterthwaite approximation to derive corrected degrees of freedom. Second, we used log-likelihood ratio tests between nested models to test for relevance of factors (e.g. GENOTYPE or AGE). For all analyses where log-likelihood ratio tests were performed, we used the maximum likelihood (ML) method to fit the model; otherwise, we used the restricted maximum likelihood (REML) method. To correct for multiple comparisons when performing analyses across all frequencies, we additionally applied a random permutation approach (8). Specifically, for each of 10,000 resamples, the GENOTYPE label for subjects (e.g. AS, TD) was

randomly permuted. We then derived p-values for each frequency and retained only the smallest p-value across all frequencies for each resample to build a null-hypothesis distribution that accounts for multiple testing.

To evaluate stability of the delta-band EEG effect, we used the intraclass correlation coefficient derived from the first two visits of subjects with more than one visit (9, type 1-1).

For illustration and to precisely determine peak frequencies, we used spline-interpolation to derive a higher frequency resolution.

All data analyses were performed in MATLAB (The MathWorks, Inc., Torrance, California) using custom scripts, FastICA for independent component analyses (http://www.cis.hut.fi/projects/ica/fastica/, (10)), and the FieldTrip toolbox to create topographic plots (11).

Supplemental Discussion

$GABA_AR$ Hypothesis Provides Testable Predictions

Our results suggest that deletion of the *GABRB3-GABRA5-GABRG3* gene cluster underlies the electrophysiological differences between AS deletion and non-deletion genotypes. This $GABA_AR$ hypothesis provides specific, falsifiable predictions.

Haploinsufficiency per se of the *GABRB3-GABRA5-GABRG3* gene cluster should (A) be sufficient to induce the theta and beta EEG phenotypes observed in deletion AS and (B) be insufficient to induce the AS delta phenotype. In fact, a population that allows testing these hypotheses exists. Prader-Willi syndrome (PWS) is a neurogenetic disorder characterized by delayed development, hyperphagia, and obesity. This disorder is generally caused by either a paternal 15q11-q13 deletion or maternal UPD of chromosome 15 (12). Since *UBE3A* is expressed maternally, *UBE3A* expression levels in the brain are presumably normal in the PWS

deletion genotype, whereas PWS caused by maternal UPD should feature *UBE3A* overexpression. At the same time, individuals with deletion PWS (but not maternal UPD) are hemizygous for the *GABRB3-GABRA5-GABRG3* gene cluster, likely causing the same haploinsufficiency of these genes observed in deletion AS. Indeed, this speculation is supported by the finding of reduced $GABA_AR$ density in deletion PWS (13). Thus, PWS caused by 15q11-q13 deletion and maternal UPD may serve as *UBE3A* normal and *GABRB3-GABRA5-GABRG3* gene cluster normal controls groups, respectively, for testing our hypotheses. More specifically, we predict excessive theta power, deficient beta power, and normal delta power in deletion PWS. We also predict normal theta- and beta-band EEG in maternal UPD PWS. To our knowledge, there are no published EEG studies of PWS that would sufficiently address our above predictions. Future studies should therefore utilize PWS EEG to test these hypotheses.

Another avenue for testing our $GABA_AR$ hypothesis is pre-clinical experiments in knock-out animals. It has been reported that maternal *Ube3a* knockout mice have an EEG phenotype that resembles excessive low frequency oscillations seen in AS (1, 14, 15), though further work is needed to understand differences between mouse lines. DeLorey and colleagues reported abnormal EEG in a *gabrb3* knockout mouse line (16), but it remains to be established whether such mice have excessive theta and/or reduced beta-band oscillations, much less whether these mice would show all EEG features if crossed with *Ube3a* knock-out mice.

EEG as a Biomarker of AS

Understanding the AS EEG phenotype also has important practical implications for the development of treatments. To this end, it is important to understand if an EEG biomarker reflects *UBE3A*-related pathologies or pathologies related to other genes commonly deleted in AS. Our results corroborate previous work suggesting delta-band EEG power as a highly promising biomarker for AS. In particular, we provide groundwork on developmental trajectories, variances, effect sizes, genotype differences, and spatial topographies that may help in planning future studies of EEG biomarkers. Our findings provide evidence that the AS delta-band EEG abnormality indexes *UBE3A*-related pathophysiology, while the deletion AS theta-band and beta-band EEG abnormalities index contributions from other genes, most likely

GABRB3-GABRA5-GABRG3 gene cluster. Thus, the meaning and relevance of the biomarker depends on the target of the treatment. If re-expression of *UBE3A* is the main target of the treatment, EEG delta-band power should be the focus of investigation, whereas if the $GABA_AR$s are the target, theta and beta power should be the focus of investigation. As such, quantitative EEG might provide surrogate endpoints in AS clinical trials.

We characterized delta, theta, and beta power at the group-level peak frequencies identified in the power spectral density. To derive robust EEG biomarkers, broader frequency ranges around the peak frequencies may be defined (e.g. for delta: power in the range of 2.5 to 4.25 Hz). Furthermore, one might utilize an individualized biomarker approach that takes the power at or around each patient's unique peak frequency (rather than the group-level averages identified herein).

The AS EEG abnormalities in delta, theta, and beta show substantial variability across participants. Some variance may be explained by the participant's state or reflect residual technical or physiological artifacts. Nonethless, a substantial portion of the variability is likely physiological. Future work should investigate this variability and attempt to link it to symptom severity.

Supplemental Tables

	Deletion AS					Non-deletion AS					TD
	Class I	**Class II**	**Atypical**	**Unknown**	**Sum**	**Mutation**	**UPD**	**Impr.**	**Methyl.**	**Sum**	**TD**
BCH	2 (2)	10 (13)	2 (2)	1 (1)	15(18)	6 (7)	3 (3)	4 (8)	1 (1)	14 (19)	48 (48)
RCHSD	8 (11)	14 (20)	-	-	22(31)	4 (6)	1 (1)	1 (2)	1 (2)	7(11)	-
Σ	10 (13)	24 (33)	2 (2)	1 (1)	**37** (49)	10 (13)	4 (4)	5 (10)	2 (3)	**21** (30)	**48** (48)

Supplemental Table S1. Dataset overview. The final dataset analyzed included 127 recordings from 106 participants. This table breaks down participants by genotypes and recording center. The number of datasets analyzed is provided in parenthesis. This deviates from the number of participants for the AS group since longitudinal data was acquired for some participants. UPD: paternal uniparental disomy; Impr.: imprinting defect; Methyl.: abnormal DNA methylation, deletion excluded (i.e. UPD or Impr.).

Name	Estimate	SE	t-stat	DF	p-value	Lower	Upper
Intercept	22.39	0.50	45.18	117.87	$<10^{-14}$	21.41	23.37
AS	7.49	0.65	11.58	110.02	$<10^{-14}$	6.21	8.77
LogAge	-2.60	0.44	-5.94	117.87	$<10^{-14}$	-3.47	-1.73
AS:LogAge	-0.57	0.60	-0.96	116.66	0.3393	-1.75	0.61

Supplemental Table S2. AS vs TD, LMM coefficients for total power analysis (1 – 32 Hz). Fixed effects parameter for LMM POWER ~ 1 + GENOTYPE + AGE + GENOTYPE:AGE + (1|PARTICIPANT) with GENOTYPE being AS or TD and POWER being the 10·log10(BroadbandPower) where BroadbandPower is the integral over the frequency range from 1 to 32 Hz in units μV^2. SE is the standard error of the mean, DF is the degrees of freedom estimated using the Satterwaite approximation, Lower and Upper and provide the lower and upper end for 95% confidence intervals.

Name	Estimate	SE	t-stat	DF	p-value	Lower	Upper
Intercept	15.80	0.67	23.65	120.82	$<10^{-14}$	14.48	17.13
AS	11.08	0.87	12.82	112.97	$<10^{-14}$	9.37	12.79
LogAge	-3.17	0.59	-5.37	120.82	$<10^{-14}$	-4.34	-2.00
AS:LogAge	-1.03	0.80	-1.28	117.51	0.2021	-2.61	0.56

Supplemental Table S3. AS vs TD, LMM coefficients for delta peak power (2.8 Hz). Fixed effects parameter for LMM POWER ~ 1 + GENOTYPE + AGE + GENOTYPE:AGE + (1|PARTICIPANT) with GENOTYPE being AS or TD and POWER being the power spectral density at 2.8 Hz in units $10 \cdot \log10(\mu V^2/\log_2(Hz))$. SE is the standard error of the mean, DF is the degrees of freedom estimated using the Satterwaite approximation, Lower and Upper and provide the lower and upper end for 95% confidence intervals.

Name	Estimate	SE	t-stat	DF	p-value	Lower	Upper
Intercept	25.37	1.20	21.34	50.45	$<10^{-14}$	22.98	27.75
DEL_AS	2.97	1.49	2.01	50.34	0.0498	0.00	5.94
LogAge	-1.86	1.30	-1.44	59.13	0.1544	-4.44	0.72
DEL_AS:LogAge	-2.69	1.56	-1.75	60.21	0.0861	-5.78	0.39

Supplemental Table S4. Deletion vs Non-deletion AS, LMM coefficients for delta peak power (2.8 Hz). Fixed effects parameter for LMM POWER ~ 1 + GENOTYPE + AGE + GENOTYPE:AGE + (1|PARTICIPANT) with GENOTYPE being deletion AS or non-deletion AS and POWER being the power spectral density at 2.8 Hz in units $10 \cdot \log10(\mu V^2/\log_2(Hz))$. SE is the standard error of the mean, DF is the degrees of freedom estimated using the Satterwaite approximation, Lower and Upper and provide the lower and upper end for 95% confidence intervals.

Name	Estimate	SE	t-stat	DF	p-value	Lower	Upper
Intercept	12.95	0.55	23.88	47.77	$<10^{-14}$	11.86	14.04
DEL_AS	-1.67	0.68	-2.48	47.82	0.0168	-3.03	-0.32
LogAge	-1.33	0.58	-2.31	58.43	0.0242	-2.48	-0.18
DEL_AS:LogAge	0.13	0.69	0.19	61.48	0.8517	-1.24	1.50

Supplemental Table S5. Deletion vs Non-deletion AS, LMM coefficients for beta peak power (23 Hz). Fixed effects parameter for LMM POWER ~ 1 + GENOTYPE + AGE + GENOTYPE:AGE + (1|PARTICIPANT) with GENOTYPE being deletion AS or non-deletion AS and POWER being the power spectral density at 23 Hz in units $10 \cdot \log10(\mu V^2/\log_2(Hz))$. SE is the standard error of the mean, DF is the degrees of freedom estimated using the Satterwaite approximation, Lower and Upper and provide the lower and upper end for 95% confidence intervals.

Name	Estimate	SE	t-stat	DF	p-value	Lower	Upper
Intercept	20.76	0.92	22.80	50.70	$<10^{-14}$	18.94	22.59
DEL_AS	5.17	1.14	4.57	50.78	3.0·10-5	2.90	7.45
LogAge	-1.27	0.95	-1.34	62.60	0.1847	-3.16	0.62
DEL_AS:LogAge	-0.99	1.13	-0.88	66.21	0.3812	-3.23	1.25

Supplemental Table S6. Deletion vs Non-deletion AS, LMM coefficients for theta peak power (5.3 Hz). Fixed effects parameter for LMM POWER ~ 1 + GENOTYPE + AGE + GENOTYPE:AGE + (1|PARTICIPANT) with GENOTYPE being deletion AS or non-deletion AS and POWER being the power spectral density at 5.3 Hz in units $10 \cdot \log10(\mu V^2/\log_2(Hz))$. SE is the standard error of the mean, DF is the degrees of freedom estimated using the Satterwaite approximation, Lower and Upper and provide the lower and upper end for 95% confidence intervals.

Supplemental Figures

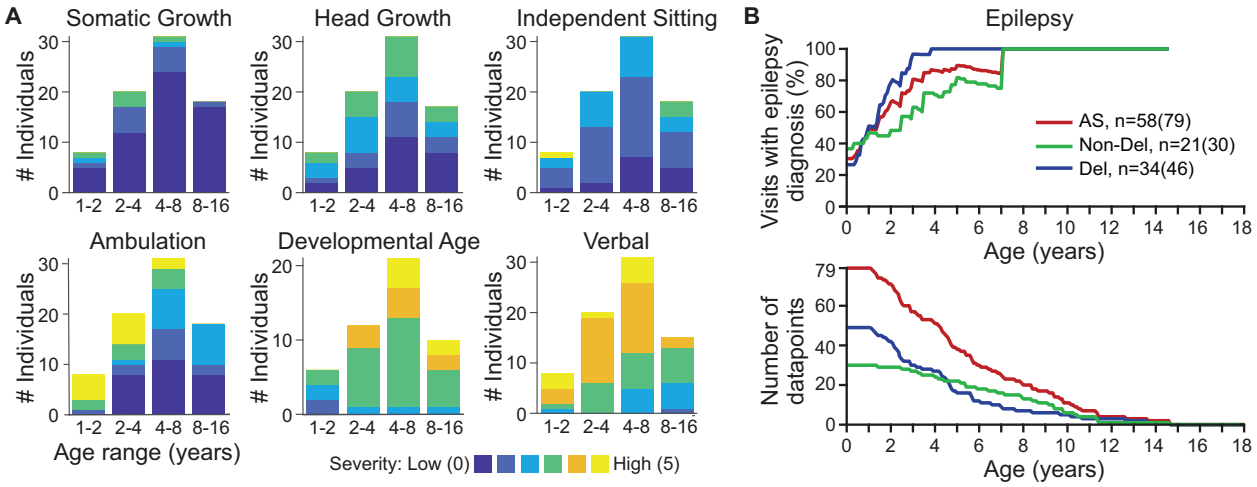

Supplemental Figure S1. Clinical presentation of individuals with AS that entered EEG analysis. (A-F) Clinical presentation in different symptom domains for AS as evaluated by study physicians. Data is split into 4 age groups. (A) Somatic growth (weight relative to TD age norms), 0: No growth failure, 1: decrease in weight > 1 SD (10%<w<25%), 2: decrease in weight > 2 SD (3%<w<10%); 3: decrease in weight > 3 SD, 4: decrease in weight > 4 SD; (B) Head growth (head circumference relative to TD age norms), 0: >25%, 1: 11-25%, 2: 2-10%, 3: <2%; (C) Independent sitting, 0: Sits alone acquired <8 months, 1: Sit with delayed acquisition (9 to 17 months), 2: Sit with delayed acquisition (18 to 30 months), 3: Sit with delayed acquisition >30 months, 4: Lost, 5: Never acquired; (D) Ambulation, 0: Acquired <18 months / Ataxic gait, 1: Walks alone 18-30 months, 2: Walks alone >30 months, 3: Walks with assistance >30 months, 4: Lost, 5: Never acquired; (E) Developmental age (derived from TD age norms of the Cognition domain of the Bayley Scales of Infant and Toddler Development – Third Edition (17)), 0: Appropriate for age to 0.5 SD below mean, 1: 0.6 – 1.5 SD below mean, 2: 1.6 – 2.5 SD below mean, 3: 2.6 – 3.5 SD below mean, 4: 3.6 – 4.5 SD below mean, 5: > 4.5 SD below mean; (F) Verbal Language, 0: phrase speech, 1: >10 single words, 2: up to 10 single words, 3: no words, babbling (vowels/consonants strung together), 4: grunts & non-word utterances (vowels only), 5: No vocalization. (G) Developmental trajectory of epilepsy in individuals with AS. Upper: Fraction of study visits with individuals that had an epilepsy diagnosis prior to a given age. At the time of the visit, for 22 of 79 visits (28%), participants had never had a seizure (all deletion AS had epilepsy by the age of 4, all non-deletion AS had epilepsy by the age of 7). For 28 of 79 visits (35%) participants had active seizures around the time of the visit (note only interictal EEG is analyzed). Lower: Number of datasets that was available to derive the upper plot.

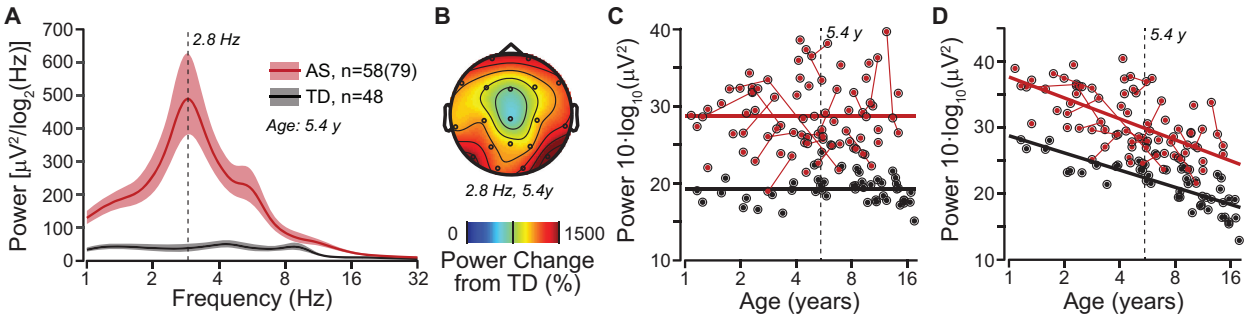

Supplemental Figure S2. Spectral power differences between AS and TD controls. (A) Grand averaged power spectral density derived from the LMM with age set to mean log age of 5.4 years (average across all visits and electrodes). Same as Figure 2A but with power instead of log-power scaling. AS: red, TD controls: black. The colored bands show 95% confidence intervals. (B) Scalp topography of power change in percent change from TD controls derived from the LMM for 2.8 Hz (i.e., AS delta peak frequency) and the mean log age of 5.4 years. (C) Developmental trajectory of channel averaged delta power (2.8 Hz) derived from the LMM as in Figure 2D but corrected for age within each group. Longitudinal visits are connected by solid lines. The intraclass correlation coefficient (ICC) derived from individuals with AS that had at least two EEGs (using the first two EEGs only) was 0.68 (95% confidence interval: 0.31 to 0.88). This indicates moderate stability. Notably, the contribution of test-retest variability and developmental changes over time (12.9 ± 3.11 month, mean ± std, range 9 to 24 month) cannot be disentangled. (D) Analysis of total power (power in the frequency range 1 – 32 Hz). Developmental trajectory: TD: -2.60 dB/oct, 95% confidence interval: -3.47 to -1.73; $p = 2.96 \times 10^{-8}$; AS: -3.17 dB/oct, 95% confidence interval: -3.97 to -2.37; $p = 2.34 \times 10^{-12}$. The slopes did not significantly differ between AS and TD controls: -0.57 dB/oct (95% confidence interval: -1.75 to 0.61; p = 0.339). See Supplemental Table S2 for further details on statistical analysis.

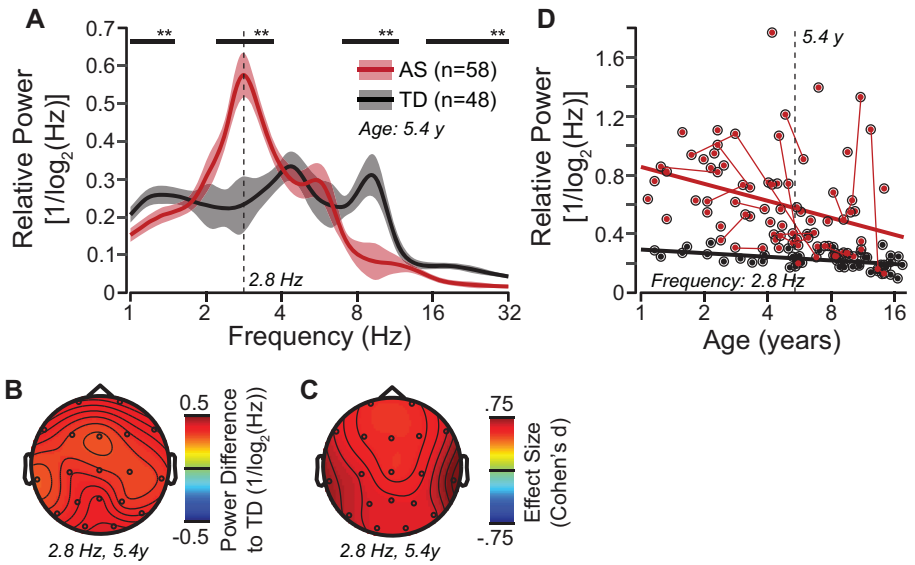

Supplemental Figure S3. Spectral differences of relative power between AS and TD controls. (A) Grand averaged power spectral density for relative power derived from the LMM with age set to the mean log age of 5.4 years (average across all electrodes). AS: red, TD controls: black. The colored bands show 95% confidence intervals. The black bars indicate frequency ranges with significant group differences (corrected for multiple testing across frequencies). (B,C) Scalp topography of relative power difference and effect size (Cohen's d) between AS and TD controls derived from the LMM for 2.8 Hz (i.e., AS delta peak frequency) and the mean log age of 5.4 years. (D) Developmental trajectory of channel averaged relative delta power (2.8 Hz) derived from the LMM. Longitudinal visits are connected by solid lines. Developmental trajectory: TD: -0.02 1/oct, 95% confidence interval: -0.09 to 0.04; p = 0.459; AS: -0.17 1/oct, 95% confidence interval: -0.17 to -0.06; p = 1.88 x 10^{-4}. The slopes did differ significantly between AS and TD controls: -0.09 1/oct (95% confidence interval: -0.18 to 0.00; p = 0.042).

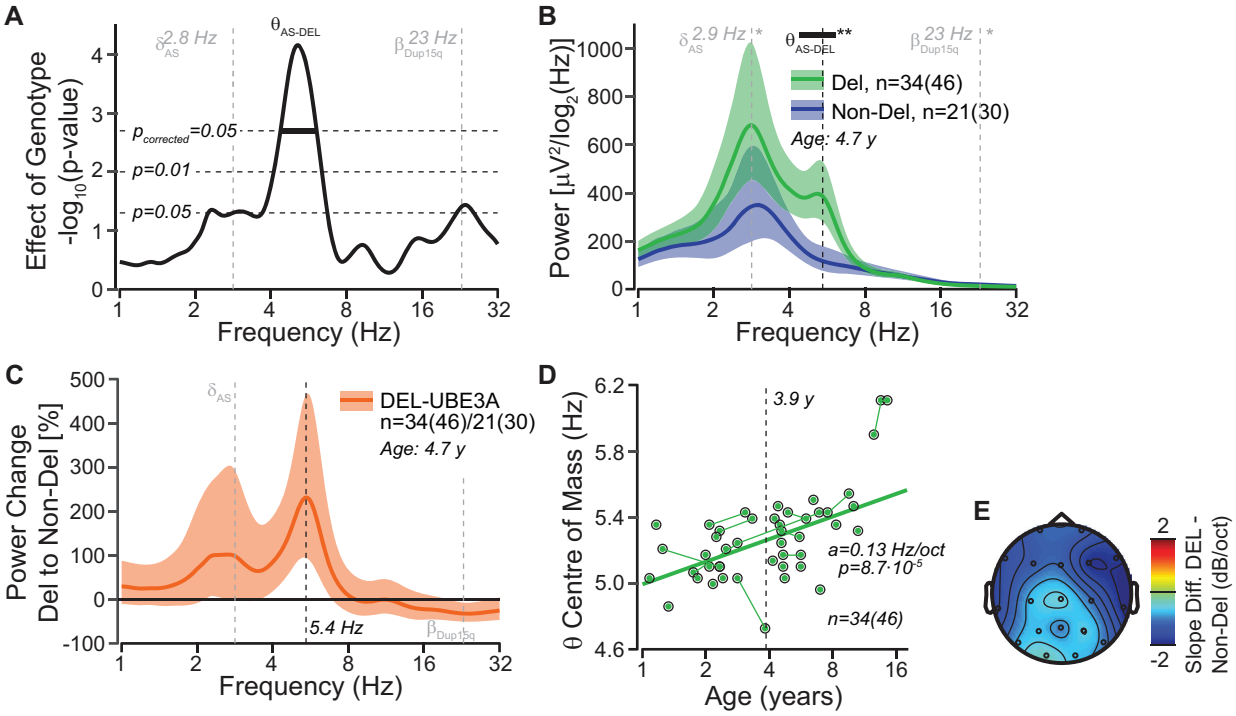

Supplemental Figure S4. Spectral power differs between AS genotypes. (A) P-values for model comparisons (log-likelihood ratio tests) between models with and without AS genotype information (see Methods section). The horizontal lines depict different statistical threshold with and without correction for multiple testing across frequencies. (B) Grand average power spectral density derived from the LMM with age set to the mean log age of 4.7 years (average across all visits and electrodes). Same as Figure 3A but with power instead of log-power scaling. Deletion AS: green, non-deletion AS: blue. The colored bands show 95% confidence intervals. The black bar indicates frequency ranges with significant group differences (corrected for multiple testing across frequencies). The gray lines indicate the specific hypotheses tested in the delta and beta bands (see Figures 3 and 4). (C) Difference in spectral power of deletion AS relative to non-deletion AS in percent change. The colored bands show 95% confidence intervals. The gray lines indicate the specific hypotheses tested in the delta and beta bands (see Figures 3 and 4). (D) Correlation between age and the center of mass of electrode averaged power in the theta frequency range (alternative metric to peak frequency, see Figure 5D). (E) Scalp topography of difference in developmental changes between deletion AS and non-deletion AS (i.e. difference of slopes of power change with age in $10 \cdot \log_{10}(\text{Pow})/\text{oct}$), derived from the LMM for 5.3 Hz and the mean log age of 4.7 years.

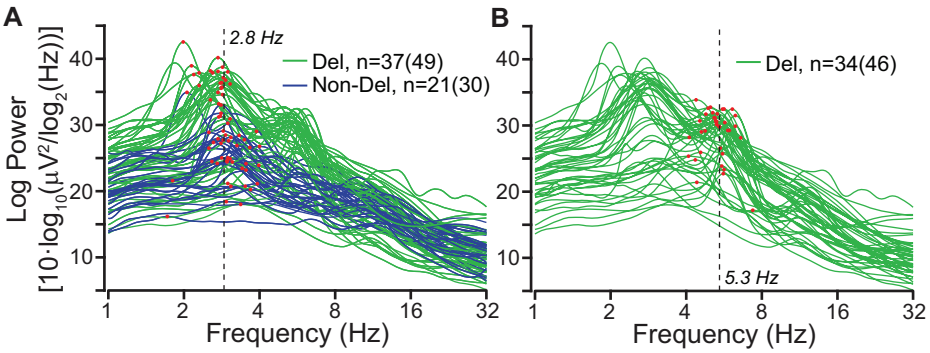

Supplemental Figure S5. Individually labeled spectral peaks on channel averaged power spectral densities from AS participants (labeling was performed separately for each visit in longitudinal data). Spectral peaks were manually labeled in the delta and theta frequency bands. If manually selected frequency values differed from an automatic approach using the local maximum by less than 5%, the automatic peak label was used instead. (A) Individually labeled delta (1.5 – 4 Hz) peaks indicated by red dots on spectra from participants with the AS deletion genotype (green) and the AS non-deletion phenotype (blue). We identified delta peaks in 70 of 79 recordings from 54 of 58 participants. (B) Individually labeled theta (4- 8 Hz) peaks indicated by red dots on spectra from participants with the AS deletion genotype (green) with atypical and unknown deletions excluded. We identified theta peaks in 37 of 46 recordings from 28 of 34 participants with deletion AS (only class I and class II are considered).

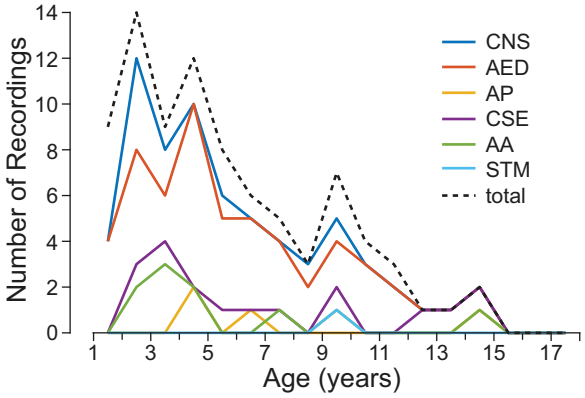

Supplemental Figure S6. Medication as a function of age. Six different medications types: CNS: Central Nervous System; AED: Antiepileptic Drug; AP: Antipsychotic; CSE: CNS Side Effects; AA: Alpha Agonist; STM: Stimulant. The total number of available recordings in a given age bin is indicated by the black dotted line.

Supplemental References

1. Sidorov MS, Deck GM, Dolatshahi M, Thibert RL, Bird LM, Chu CJ, Philpot BD (2017): Delta rhythmicity is a reliable EEG biomarker in Angelman syndrome: a parallel mouse and human analysis. *J Neurodev Disord*. 9: 17.
2. Vendrame M, Loddenkemper T, Zarowski M, Gregas M, Shuhaiber H, Sarco DP, *et al.* (2012): Analysis of EEG patterns and genotypes in patients with Angelman syndrome. *Epilepsy Behav*. 23: 261–265.
3. Hyvarinen A (1999): Fast ICA for noisy data using Gaussian moments. (Vol. 5), Presented at the Circuits and Systems, 1999. ISCAS'99. Proceedings of the 1999 IEEE International Symposium on, IEEE, pp 57–61.
4. Jung T-P, Makeig S, Westerfield M, Townsend J, Courchesne E, Sejnowski TJ (2000): Removal of eye activity artifacts from visual event-related potentials in normal and clinical subjects. *Clin Neurophysiol*. 111: 1745–1758.
5. Tallon-Baudry C, Bertrand O, Delpuech C, Pernier J (1997): Oscillatory γ-band (30–70 Hz) activity induced by a visual search task in humans. *J Neurosci*. 17: 722–734.
6. Buzsáki G, Draguhn A (2004): Neuronal oscillations in cortical networks. *Science*. 304: 1926–1929.
7. West BT, results search, results search (2014): *Linear Mixed Models: A Practical Guide Using Statistical Software, Second Edition*, 2 edition. Boca Raton: Chapman and Hall/CRC.
8. Nichols TE, Holmes AP (2002): Nonparametric permutation tests for functional neuroimaging: a primer with examples. *Hum Brain Mapp*. 15: 1–25.
9. McGraw KO, P S (1996): Forming inferences about some intraclass correlation coefficients. *Psychol Methods*. 1: 30–46.
10. Hyvarinen A (1999): Fast and robust fixed-point algorithms for independent component analysis. *IEEE Trans Neural Netw*. 10: 626–634.
11. Oostenveld R, Fries P, Maris E, Schoffelen J-M (2011): FieldTrip: open source software for advanced analysis of MEG, EEG, and invasive electrophysiological data. *Comput Intell Neurosci*. 2011: 1.
12. Cassidy SB, Driscoll DJ (2009): Prader–Willi syndrome. *Eur J Hum Genet*. 17: 3.

13. Lucignani G, Panzacchi A, Bosio L, Moresco RM, Ravasi L, Coppa I, *et al.* (2004): GABAA receptor abnormalities in Prader–Willi syndrome assessed with positron emission tomography and [11C]flumazenil. *NeuroImage*. 22: 22–28.
14. Born HA, Dao AT, Levine AT, Lee WL, Mehta NM, Mehra S, *et al.* (2017): Strain-dependence of the Angelman Syndrome phenotypes in Ube3a maternal deficiency mice. *Sci Rep*. 7: 8451.
15. Judson MC, Wallace ML, Sidorov MS, Burette AC, Gu B, van Woerden GM, *et al.* (2016): GABAergic neuron-specific loss of Ube3a causes Angelman syndrome-like EEG abnormalities and enhances seizure susceptibility. *Neuron*. 90: 56–69.
16. DeLorey T, Handforth A, Anagnostaras S, Homanics G, Minassian B, Asatourian A, *et al.* (1998): Mice lacking the β3 subunit of the GABAA receptor have the epilepsy phenotype and many of the behavioral characteristics of Angelman syndrome. *J Neurosci*. 18: 8505–8514.
17. Albers CA, Grieve AJ (2007): Test Review: Bayley, N. (2006). Bayley Scales of Infant and Toddler Development– Third Edition. San Antonio, TX: Harcourt Assessment. *J Psychoeduc Assess*. 25: 180–190.